Journal of Thermal Analysis and Calorimetry (2022) 147:7509–7521
https://doi.org/10.1007/s10973-021-11002-y

Improve the heat exchanger efficiency via examine the Graphene Oxide nanoparticles: a comprehensive study of the preparation and stability, predict the thermal conductivity and rheological properties, convection heat transfer and pressure drop

Ramin Ranjbarzadeh[1] · Alireza Akhgar[2] · Roozbeh Taherialekouhi[2] · Annunziata D'Orazio[3] · S. Mohammad Sajadi[4,5] · Ferial Ghaemi[6] · Dumitru Baleanu[7,8,9]

Received: 18 May 2021 / Accepted: 9 July 2021 / Published online: 22 August 2021
© Akadémiai Kiadó, Budapest, Hungary 2021

Abstract
In this research, the effect of using GO/ water nanofluid as a coolant fluid in an isothermal heat transfer system was studied. At first, to evaluate the atomic bond, chemical, and surface structure of the nanoparticles, XRD-FTIR and FESEM tests were used. Two-step method was used to prepared nanofluid then DLS test was utilized to examine the stability of the nanofluid. Thermal conductivity and the dynamic viscosity were measured experimentally from 25 to 75 ℃ and volume fractions of 0–0.15%. The maximum improvement in thermal conductivity is 11.2% at 0.15% and 75 ℃. Also The dynamic viscosity increased. The validity and uncertainty of the test results were examined. The heat transfer and turbulent flow of the nanofluid under a constant temperature boundary condition were investigated between 6000 and 18,700 Reynolds numbers. Various parameters such as the pressure drop, friction factor, convection heat transfer coefficient, and Nusselt number of the turbulent flow were evaluated. According to the results, the greatest increase in the convection heat transfer coefficient of the nanofluid was 34.7% compared to that of the base fluid. Also, the greatest enhancement in the friction factor was 9.64%. It can be stated that the improvement of the convection heat transfer coefficient dominantly affects the pressure drop so this nanofluid can be used as a coolant fluid in industrial systems.

Keywords Stabilize · Pressure drop · Turbulent flow · Heat transfer

Introduction

Limitations of energy resources in recent decades have highlighted the necessity of energy saving. The employment of engineering approaches in the optimization of energy consumption and the improvement of heat transfer has always been a positive approach for enhancing the efficiency of thermal systems. According to the importance of heat transfer matter in industry, designers and researchers always seek a new idea to improve the performance of

✉ Dumitru Baleanu
dumitru@cankaya.edu.tr

[1] Department of Civil, Constructional and Environmental Engineering, Sapienza University of Rome, Via Eudossiana 18, 00184 Rome, RM, Italy

[2] Department of Mechanical Engineering, Khomeinishahr Branch, Islamic Azad University, Khomeinishahr, Iran

[3] Department of Astronautics, Electrical and Energetics Engineering, Sapienza University of Rome, Via Eudossiana 18, 00184, Rome, RM, Italy

[4] Department of Nutrition, Cihan University-Erbil, Kurdistan Region, Erbil, Iraq

[5] Department of Phytochemistry, SRC, Soran University, KRG, Soran, Iraq

[6] Department of Chemical and Process Engineering, Faculty of Engineering and Built Environment, Universiti Kebangsaan Malaysia (UKM), 43600 Bangi, Selangor, Malaysia

[7] Department of Mathematics, Faculty of Arts and Sciences, Cankaya University, Ankara, Turkey

[8] Institute of Space Sciences, Magurele, Romania

[9] Department of Medical Research, China Medical University Hospital, China Medical University, Taichung, Taiwan

heat exchangers by different methods such as using baffles and turbulators, designing an optimum geometric shape, changing laminar flow to turbulent flow and taking advantage of the benefits of turbulent flow in the improvement of heat transfer, etc. [1–4].

One of the approaches considered by researchers in this field is using nanofluid instead of common fluids such as oil, water and ethylene glycol, etc. in thermal systems. In this case, metallic materials, metal oxide, carbon-based materials, etc. with nanometer size and higher thermal conductivity properties are dispersed in the base fluid, then a nanofluid with a higher thermal conductivity compare to the base fluid is prepared which improves the heat transfer coefficient significantly [5–9].

Choi introduced nanofluids for the first time in 1995[10]. Numerous experimental and numerical simulation studies have been performed by researchers during recent years in this field to improve the performance of heat transfer and investigate the effect of various factors such as the nanoparticles type, volume fraction, method of nanofluid synthesis, a temperature range of the nanofluid flow, Reynolds number on the improvement of heat transfer. Some of these factors are evaluated in the last studie regarding the Graphene oxide [11, 12].

Bashirnezhad et al. [13] investigated the improvement of convection heat transfer by using nanofluids containing TiO_2, CuO and Al_2O_3 metal oxide nanoparticles and evaluated the effective different parameters on convection heat transfer and thermal conductivity including the volume fraction of the different nanoparticles, Reynolds number, Nusselt number, Rayleigh number. The results show that convection heat transfer and thermal conductivity are improved. It should be mentioned that Shah's classical model had not a high accuracy in predicting convection heat transfer of nanofluids.

Kung Ki et al. [14] investigated the performance of heat transfer and pressure drop of the TiO_2/water nanofluid in a double tube- heat exchanger. Various factors including the volume flow rate, the volume fraction, the Reynolds number and the internal structure of the exchanger are investigated in this research. The results showed that the nanofluid is capable of improving the heat conduction by 10.8% to 14.8% compared to the water base fluid. In addition, the nanofluid compared to water has led to a pressure drop of 51.9% on the tube side and a pressure drop of 40.7% on the shell side.

Sadeghinezhad et al. [15] evaluated the thermal performance of graphene/water nanofluid in a heat pipe. This study is performed by focusing on the effect of the nanofluid volume fractions and the slope angle of the heat pipe inside the heat source. The maximum reduction in its thermal resistance is observed to be 48.4% compared to the water.

Ranjbarzadeh et al. [16] investigated the effect of using nanofluid in a thermal system. The volume fractions of nanofluid samples are in the range of 0 to 0.1 percent and the Reynolds number of turbulent flow is in the range of 5250 to 36,500. The maximum increase in the thermal conductivity compared to the base fluid is 27.5%. Furthermore, the convection heat transfer coefficient of the nanofluid increased to 38.9% compared to the base fluid. Also, the friction factor increased to 15.1% compared to the base fluid that has resulted in a negligible pressure drop.

Prasad et al. [17] used a nanofluid containing alumina nanoparticles to improve the heat transfer in a U-shaped heat exchanger containing twisted tape insert. The volume fractions of the nanoparticles used in the base fluid were 0.01 and 0.03 percent. In this research, the Nusselt number has increased throughout the tube for a volume fraction of 0.03 percent by 31.28% compared to water.

Yarmand et al. [18] studied the effect of using a nanofluid containing graphene nanosheets. Different parameters such as the thermo-physics properties of the graphene nanofluid, the friction factor and the heat transfer coefficient of the fluid flow in a square tube with constant heat flux wall were investigated. At volume fraction of 0.1% and Reynolds number of 17,500, the greatest improvement in the total heat transfer coefficient and the Nusselt number was observed to be 19.68% and 26.5% respectively while the friction factor increased by 9.22% at this volume fraction.

Devireddy et al. [19] experimentally studied the influence of the water- ethylene glycol/ TiO2 nanofluid as a coolant fluid in an air-cooled exchanger. The heat transfer coefficient of the nanofluid was investigated in 0.1% to 0.5% volume fraction. All experiments were performed in a range of Reynolds numbers from 4000 to 15,000. The improvement of the heat transfer increased to 37% compared to the base fluid in a range of Reynolds numbers between 4000 and 15,000.

Kumar et al. [20] investigated the effect of two nanofluids on heat transfer in a plate heat exchanger. ZnO/water and CeO_2/water nanofluids are used individually in this research. The nanofluid containing zinc oxide nanoparticles had a better performance compared to the other one. The nanofluid containing Zinc oxide nanoparticles increased HTR and HTC by 5.12% and 12.79% respectively compared to the nanofluid containing CeO_2.

Sarafraz et al. [21] experimentally studied the performance of a copper heat sink with a rectangular microchannel using Ag/ water nanofluid as a coolant. Different parts such as pressure drop, friction factor and thermal resistance were examined experimentally at volume fractions of 0.01, 0.05 and 0.1 percent. The results reveal that the thermal conductivity and the pressure drop increased. Accordingly, there is a reduction in the total thermal resistance along the microchannel. The optimal concentration of the silver

nanofluid was 0.05 mass percent and improved the total thermal performance of the system by 37% at a Reynolds number of 1400.

Kumar et al. [22] investigated the friction factor and the convection heat transfer of the Fe_3O_4/water nanofluid in a double tube heat exchanger. The volume fraction of the nanoparticles used in this experiment was in the range of 0.005% to 0.06% and the Reynolds number was in the range of 15,000 to 30,000. According to the obtained results, the Nusselt number improved by 14.7% compared to water.

The main objective of this experimental research is to evaluate the improvement of heat transfer in an applied system by using Graphene oxide/ water nanofluid and investigate the stability of nanofluid that prepare by means of two-step method. Heat transfer, Nusselt number, pressure drop and friction factor are investigated in different variables such as temperature, volume fractions and Reynolds number. In this comprehensive study, we will investigate different parts including characterization of nanoparticles, preparation, stability, flow and heat transfer properties in deep and clarify the effect of each part on this improvement.

Objective of the study

The thermal properties of the nanofluid as the most important intended parameter are experimentally measured under different various temperature and at volume fractions of 0–0.04–0.08–0.16. Then the effect of using this nanofluid as a coolant is examined under the influence of various variables such as the volume fraction and the Reynolds number. The main parameters are heat transfer and fluid flow under a constant temperature boundary conditions. The range of Reynolds number in this experiment is from 6100 to 18,700 and the coolant flow enters the copper tube of the test at ambient temperature and absorbs the heat embedded in the tube wall as it passes through the tube. This study is based on improving the heat transfer performance in an industrial system, according to the volumetric flow rate, the research is studied in this Reynolds number range. The details and mechanisms of the test system are presented in the following sections. The results of this research will include the investigation of the stability and thermophysical properties of the nanofluid. Appropriate experimental relationships will be presented for the variables of interest by using the results of this experiment.

A comprehensive investigation about the preparation process of nanofluid, stability, characterization of nanoparticles, measurement of thermal properties, convection heat transfer, and pressure drop in a constant temperature thermal heat exchanger s carried out in this research. The other necessary details are reported in the following.

Experimental system

Figure 1 illustrates the schematic of the experimental system. The experimental system is composed of a closed-loop heat transfer cycle that consists of various segments including a nanofluid tank, a circulation pump, a flowmeter, a copper tube for the test section, a differential pressure gauge, five numbers K-type thermocouple with the thermometer, some heating element for evaporating water in the test section, and jointing tubes. The thermal stable state for recording the experimental data is about 15 min after the establishment of the flow in the experimental cycle. All experiments are repeated at least two times.

Preparation of the nanofluid

In this research a high- purity Graphene Oxide nanoparticle that produces by US Research Nanomaterials, Inc. was used. The two-step method is the best approach to prepare the Graphene oxide/ water nanofluid since the quality of the nanoparticles used directly affects the performance of the nanofluid. The mass of nanoparticles at different samples were calculated by Eq. 1 according to the volume fraction of the nanofluid and a digital balance (Model Number: ES-600) with high accuracy ($\pm 0.1mg$). During the process of using a IKA magnetic stirrer hot plate (IKA-4240201), nanoparticles were added to water; Then, a ultrasonic device was utilized for 30 min in order to achieve a homogeneous nanofluid, in this process we used a UP400St Ultrasonicate by a powerful 400 watts and 24 kHz. The Sonotrode S24d22D was used and Due to the heat generated during the use of the ultrasonic device, this process is done intermittently. In order to examine the stability, sedimentation photograph capturing used, then a DLS test was utilized for a more accurate examination.

$$\phi = \frac{(\frac{m}{\rho})_{GO}}{(\frac{m}{\rho})_{GO} + (\frac{m}{\rho})_{H_2O}} * 100 \quad (1)$$

KD2 Pro thermal property analyzer (Decagon Devices Inc., USA) was used for measuring the thermal conductivity of different samples. This analyzer works base on the transient hot-wire technique. In this research we used KS-1 sensor to measure thermal conductivity. Finally, each test was repeated three times to ensure the accuracy of the results. For temperature stability, samples are placed in a water bath with a 0.1 °C accuracy to measure the thermal conductivity.

The viscosity was measured by using Brookfield Viscometer (DV2EXTRA-Pro). Temperature has a direct and important effect on viscosity, a high- accuracy water circulating system (LAUDA Alpha RA 8 water bath) was used to control and fix the temperature.

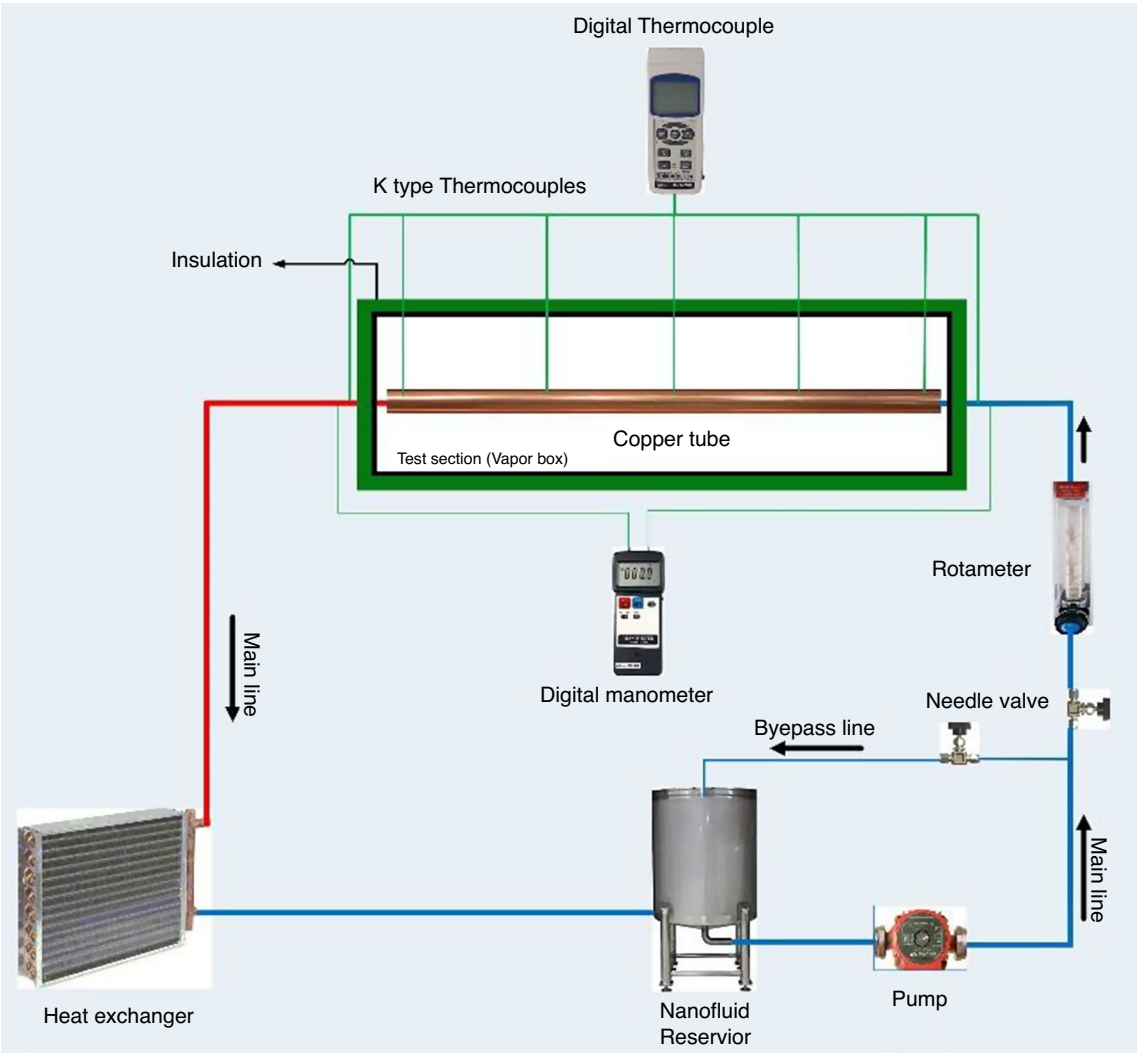

Fig. 1 Schematic of the experimental system

Governing equations

Governing equations for evaluation of fluid flow and heat transfer in a tube under constant temperature boundary conditions are presented in the following. Convection heat transfer part is the dominant mode of heat transfer in this experimental system according to the governing physics of the problem.

Equation 2 is used to calculate the convection heat transfer coefficient [23]:

$$h = \frac{\rho Q C_{\mathrm{p}} \left(T_{\mathrm{out}} - T_{\mathrm{in}}\right)}{\pi D L \Delta T_{\mathrm{LMTD}}} \tag{2}$$

In the present research, the most significant properties of GO/water nanofluid include thermal conductivity and viscosity are measured experimentally. The other properties including ρ and C_p are calculated by using Eqs. (3) and (4) presented by Pak and Cho [24]. According to previous studies, there is not significant change for specific heat capacity and density properties by increasing temperature and volume fraction in most Nanofluids [7]. Therefore, these equations have been proposed in various studies to calculate these values.

$$\rho_{\mathrm{nf}} = \phi \rho_{\mathrm{np}} + (1 - \phi)\rho_{\mathrm{f}} \tag{3}$$

$$C_{\mathrm{P,nf}} = \phi C_{\mathrm{p,np}} + (1 - \phi) C_{\mathrm{p,f}} \tag{4}$$

Equations (5) and (6) are used to calculate the values of T_{S} and ΔT_{LMTD}

$$T_S = \frac{(T_1 + T_2 + T_3 + T_4 + T_5)}{5} \tag{5}$$

$$\Delta T_{LMTD} = \frac{T_{out} - T_{in}}{Ln\left((T_s - T_{in})/(T_s - T_{out})\right)} \tag{6}$$

where T_1, T_2, T_3, T_4, T_5 are temperature of surface and its logarithmic nature is related to the exponential nature in similar situations [25].

Nusselt number and the Prandtl number are calculated By using Eqs. (7) and (8):

$$Nu = \frac{hD}{K} \tag{7}$$

$$Pr = \frac{c_p.\mu}{k} \tag{8}$$

Pressure drop and heat transfer in nanofluids flow are two essential parameters specially for industrial systems. A differential pressure gauge was used between the inlet and outlet of the test section. In general, the Darcy-Weisbach equation can be used to examine the friction factor in an incompressible fluid flow. So Eqs. 9–11 are used for the calculations.

$$\Delta P = \rho.g.\Delta h \tag{9}$$

$$f = \frac{\Delta p}{\left(\frac{L}{d}\right)\rho\frac{v^2}{2}} \tag{10}$$

$$f = \frac{\pi^2 \rho \Delta p d^2}{8\dot{m}^2 L} \tag{11}$$

Uncertainty and Validation

The measurement errors are reduced as much as possible but it is not possible to eliminate them in different parts of the experiment and the amount of uncertainty for the results is calculated according to them, i.e., how much the results are free of certainty. The influence of the equipment error on the total uncertainty was studied based on the dispersion theory proposed by Moffat et al. [26]. The results are reported in Table 1.

The experiment results are compared to the results of open literature in order to verify the performance of the experimental system and calculations. First, experiments in case of pure water are performed and results for Nusselt number and friction factor are compared with Blasius results [25] (Eq. 12) and Dittus- Boelter results [27] (Eq. 13) respectively.

$$f = 0.3164Re^{-0.25}$$
$$\frac{l}{d} \geq 10 \quad 0.6 < Pr < 100 \quad 2500 < Re < 1.25 * 10^5 \tag{12}$$

$$Nu = 0.023Re^{0.8}Pr^{0.4}$$
$$0.7 < Pr < 500 \quad 1 < Re < 1 * 10^6 \tag{13}$$

The Eq. 12 was limited to the turbulent flow and also for Eq. 13. The comparisons are shown in Fig. 2 and Fig. 3 respectively. According to Fig. 2, the excellent consistency of the experimental results with the equation presented by Blasius is completely obvious such that the maximum deviation is 4.8%. According to the obtained results presented in Fig. 3, it can be stated that the achieved results are well consistent with the aforementioned Dittus-Boelter equation since the maximum error in the experiment is 5.8%. So the performed examinations, the overlapping of the experimental results of the friction factor and the obtained Nusselt number are acceptable.

Results and discussion

In this section, the results related to the characterization of nanoparticles, evaluation of the nanofluid stability, investigation of the pressure drop and friction factor of the nanofluid, also evaluation of the convection heat transfer and Nusselt number are presented. The effect of influential parameters will be discussed according to the governing physics and comparison with other studies.

Characterization of nanoparticles

The Field Emission Scanning Electron Microscopy (FESEM) test is employed to examine the surface structure of the nanoparticles, the results are given in Fig. 4. According to the results, the Graphene oxide nanoparticle is a sheet structure, the thickness of the sheets is in nanoscale, and their surface dimensions are greater in

Table 1 The empirical data uncertainty

Parameters	Uncertainty (%)
Convection heat transfer coefficient	5.2
Nu	5.7
Friction factor	4.2
Pressure drop	2.5

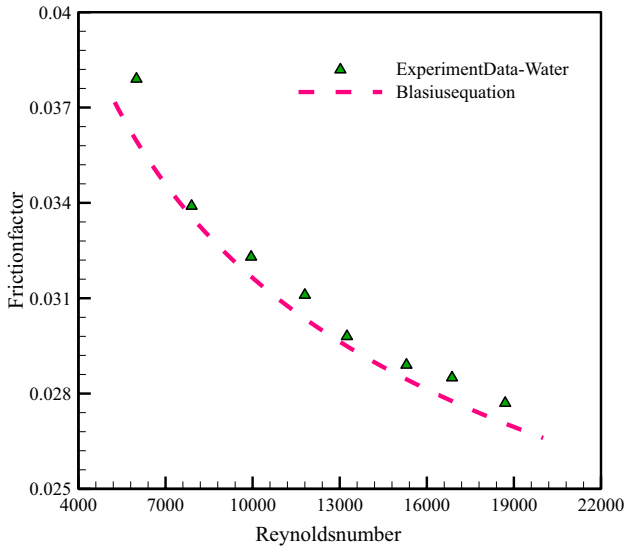

Fig. 2 Friction factor of water flow with Reynolds number

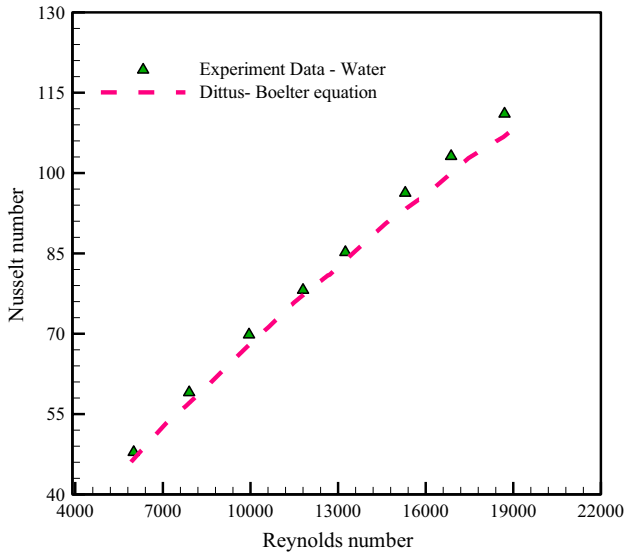

Fig. 3 Nusselt number of water flow as a function of Reynolds number

size. The results show that the surface of the nanoparticles is not smooth that results by synthesis process and the functional groups that are developed inevitably during the chemical process [28].

The X-Ray Diffraction test is utilized to examine the atomic structure of the Graphene oxide nanoparticles. The result of this test is shown in Fig. 5 that a peak is observed at $\theta = 10.4$ ° for the Graphene oxide nanoparticle that belongs to the 002 sheets of the graphene structure and complies with other references [29, 30]. In the following, Brag's equation (Eq. 14) is used to calculate the interplanar distance [31]:

$$\lambda = 2d \sin(\theta) \tag{14}$$

where d is the interplanar distance, λ the wavelength of the ray and θ the angle of the peak occurrence. The interplanar distance obtained for the graphene oxide nanoparticles is equal to 0.85 nm. Indeed, the existence of oxide groups on the Graphene oxide nanoparticles has led to an increase in the distance of the graphene sheets. This increase implies success in the oxidation process of the graphene nanosheets.

The FT-IR test is used to specify the functional groups that product in the graphene oxide nanoparticles. The FT-IR overall spectrum of these nanoparticles is depicted in Fig. 6.

According to Fig. 6, in the FT-IR test a wide peak can be observed at a wavenumber of about 3425 cm^{-1} that may be attributed to the symmetrical stretching of the OH groups of the water adsorbed to the nanofluids and nanosheets [32–48]. The peak related to the C = O bond of the carboxyl groups existing on the graphene oxide is observed at a wavenumber of 1691 cm^{-1}. The absorption peaks observable at wavenumbers of 1218 cm^{-1} and 1097 cm^{-1} in the structure of the graphene oxide correspond to the tensile bonds of the C–O and (C–O–C) epoxide groups respectively. The presence of this peak in the spectrum of the graphene oxide is another evidence for the successful oxidation of this sample.

Nanofluid stability

The stability of nanofluid is acceptable by using two-step preparation method; however the presence of the functional groups on the surface of the graphene oxide nanoparticles is a good point to make a stable condition [49–65]. Moreover, there is no big difference between the density of nanoparticle and base fluid. Choosing an appropriate process to prepare the nanofluid and using nano-dimensions particles in the base fluid have a valuable result for the established stability. The Dynamic Light Scattering (DLS) test is utilized in order to examine the stability in nanoscale. The governing theory of this experiment is based on the Mai theorem [34]. The results are shown in Fig. 7 where the intensity of the laser beam is reported with respect to the size of particles.

Bigger particles diffract a greater intensity. The maximum value of the average diameter of the particles is in the range of less than 100 nm. It can be stated that the dimensions of the particles in the base fluid are in the nanoscale and no agglomeration has been formed.

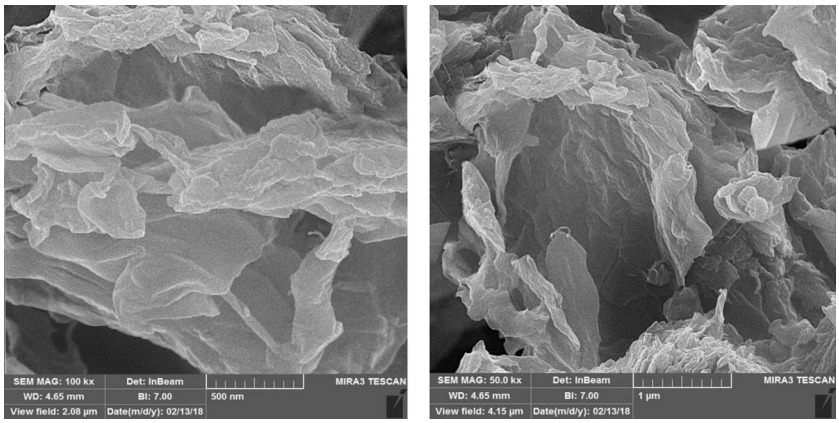

Fig. 4 FESEM image of the graphene oxide nanoparticles

Thermal conductivity and rheological behavior of the nanofluid

Figure 8 shows the thermal conductivity of Graphene oxide/water nanofluid as a function of temperature at different fractions in the temperature range of 25 to 75 degrees Celsius. The greatest value of thermal conductivity (0.742 W/m K) is observed for the highest temperature and the highest volume fraction. The thermal conductivity of the nanofluid linearly increases by increasing the volume fraction at all temperatures. The heat transfer process in the nanofluid is a relatively complex process that depends on the properties of the base fluid and the nanoparticles and their mutual effect. Furthermore, the increase in the kinetic and vibrational energy of the molecules with temperature rise and the increase in the random collisions of the particles under the effect of Brownian motion on the microscale is another effective factor for the improvement of the thermal conductivity of the nanofluid [35]. In this regard, the nanoparticles collide with each other continuously by increasing the volume fraction of the nanofluid according to reasons such as the movement of the fluid mass with the particle inertia, lift force and other transverse forces, the interparticle electrical force, interparticle mutual hydrodynamic effect, etc. and form clusters and chains of nanoparticles that lead to a greater improvement on the thermal conductivity.

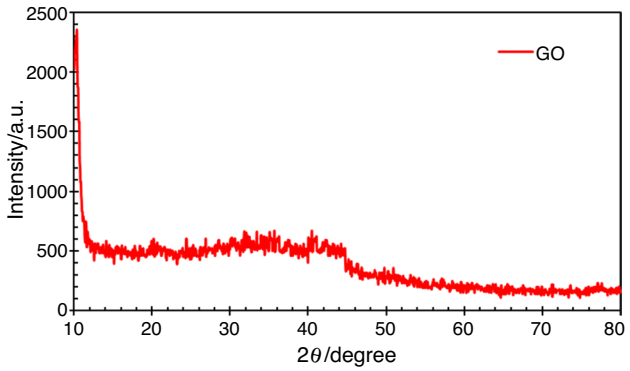

Fig. 5 XRD test for GO nanoparticle

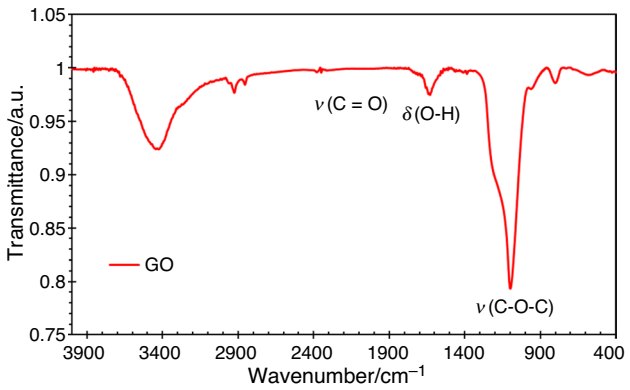

Fig. 6 FT-IR spectrum for graphene oxide nanoparticle

The rheological behavior of the nanofluid at different volume fractions is shown in Fig. 9. It can be seen that the nanofluid behavior is a Newtonian fluid, similar to the base fluid. With regard to the effect of various temperatures on the nanofluid viscosity, we report only results of the experiment at 25 and 75 degrees Celsius since similar behaviors are observed in the temperature range.

The dynamic viscosity as a function of temperature in the range of 25 to 75 degrees Celsius and for different volume fractions is given in Fig. 10. The amount of the nanofluid dynamic viscosity decreases with the temperature at a specific volume fraction and increases with the volume fraction more significantly at low temperatures. For a volume fraction equal to 0.16% and a temperature of 25 °C the dynamic viscosity is equal to 2.181 mPa s. In liquids, the molecules can overcome the intermolecular adhesive force under the effect of more energy (Under the effect of temperature rise), hence the viscosity of the nanofluid decreases as a result of temperature rise. The influence of the increase in the

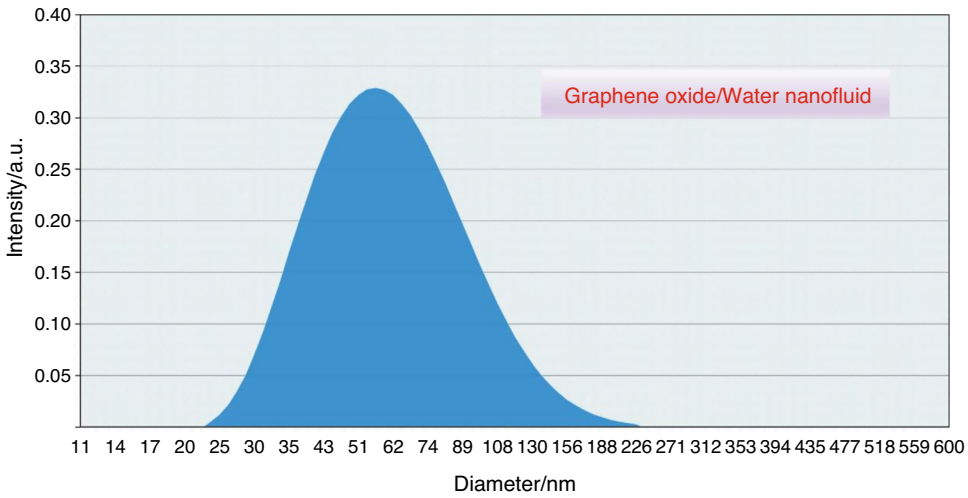

Fig. 7 DLS test for nanofluid stability examination

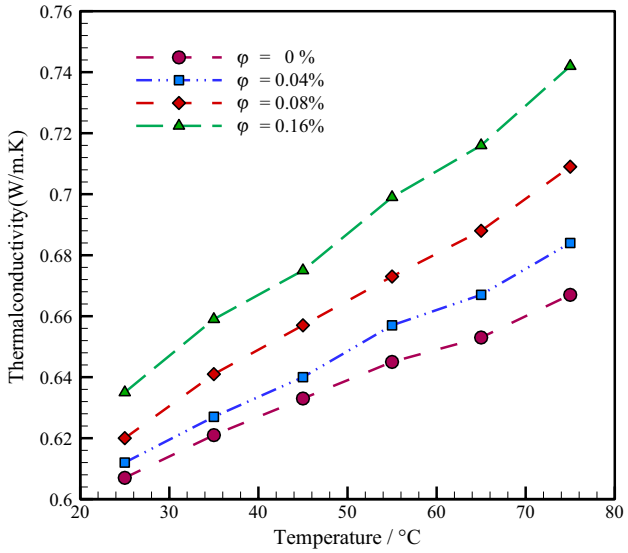

Fig. 8 Thermal conductivity versus temperature at various volume fractions

Brownian motion of the nanoparticles with temperature rise on the nanofluid viscosity is significant. Temperature rise increases the intermolecular distance of the nanoparticles and the base fluid. Therefore, the resistance against the flow and the viscosity of the nanofluid decrease.

According to the results at different temperatures, there is an increase in the amount of dynamic viscosity by increasing the volume fraction of the nanoparticles in the base fluid and this increase is attributed to the flow resistance against shear rate for various concentrations. The viscosity of water increases by adding a minor volume percent of 0.04 of the nanoparticle to it while the change of viscosity is not remarkable compared to the case of increasing the concentration to 0.16 volume percent.

Based on the results presented, the viscosity of graphene oxide nanofluid changes at the low shear rate, on the contrary in the higher amounts almost there are no changes, this trend has been observed in other experimental studies. Therefore, according to the potential of the viscometer, the measurement was performed in this range.

Result of pressure drop and friction factor

Although increasing the volume fraction of nanoparticles leads to an improvement in thermal conductivity, this increase in the number of nanoparticles can have negative effects such as pressure drop. Figure 11 shows the pressure drop along the flow path of the nanofluid as a function of the Reynolds at volume fractions in a range of Reynolds numbers between 6000 and 18,700. The increase of pressure drop with Reynolds number is approximately linear; for the same Reynolds number, the pressure drop corresponding to the maximum volume fraction of the nanoparticles is 2.4 times the value corresponding to the minimum volume fraction. This phenomenon occurs due to the friction between different layers of the flow and the physical collisions of the nanoparticles and the tube wall. Dynamic viscosity increase by increasing the number of nanoparticles in the base fluid and all these actions lead to an increase in the pressure drop. An increase in the pressure drop affects the pump, but the improvement of the thermal performance achieved by using this nanofluid is far more important and the resulted problem can be eliminated just by using a pump with a higher head. In order to identify and make applied use of the mentioned nanofluid, the changes in the pressure drop should be examined accurately and comprehensively. The results of friction factor of the nanofluid with different concentrations of 0.04–0.08–0.16 percent are shown in Fig. 12. Friction factor of the nanofluid flow increased by 9.64% compared to the base fluid.

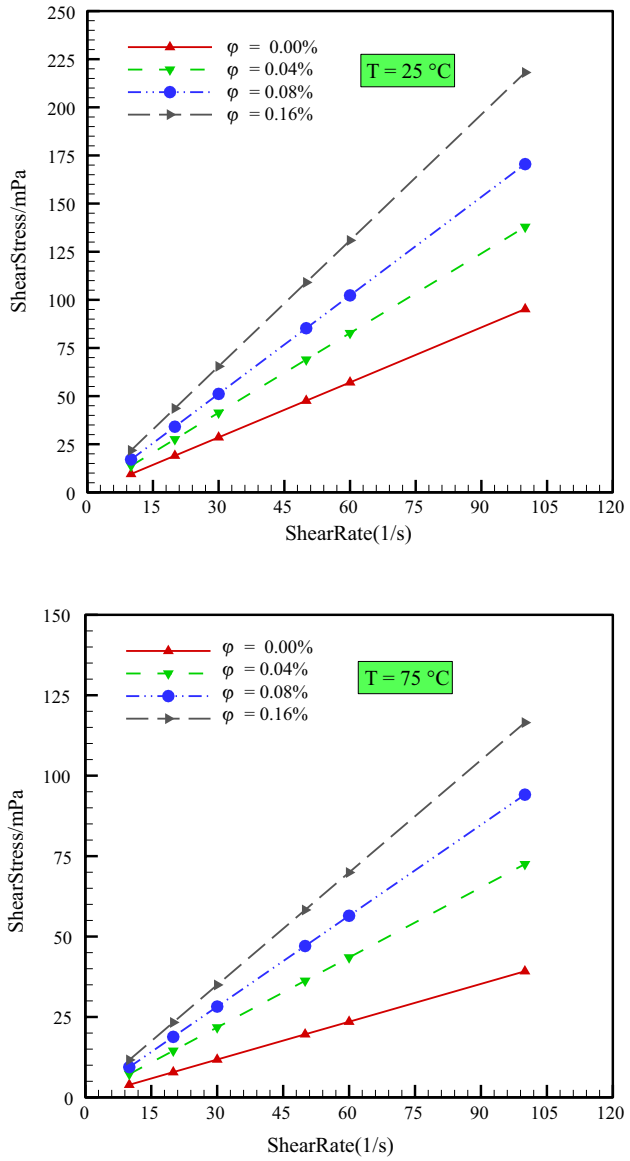

Fig. 9 Rheological behavior under the effect of shear rate at various shear stresses

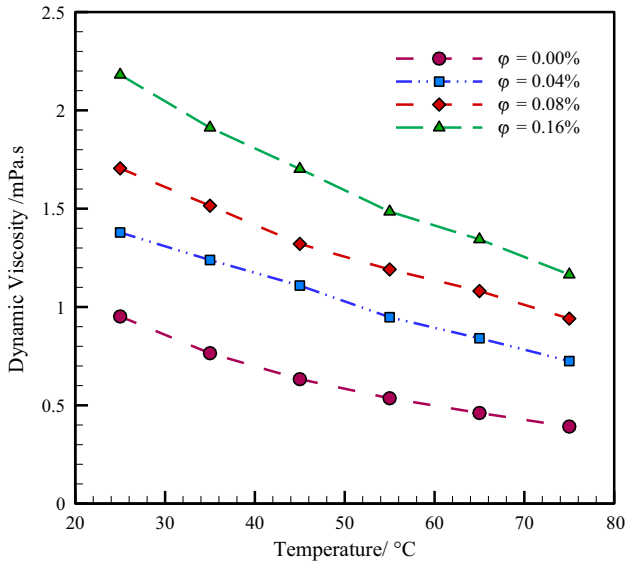

Fig. 10 Dynamic viscosity vs. temperature at various volume fractions

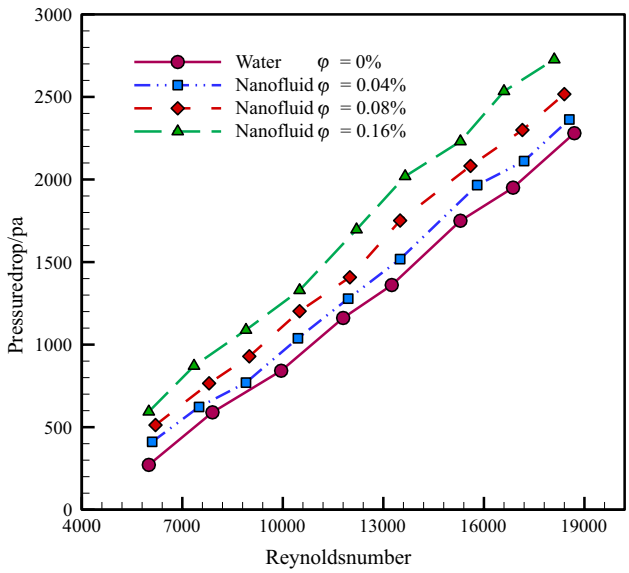

Fig. 11 Pressure drop at various Reynolds numbers

The maximum difference between the friction factor of the nanofluid and the base fluid is not significant. These changes may be attributed to the high turbulence of the flow since the perturbations resulted from the particles will be negligible compared to the flow perturbations. While the nanofluid flow through the pipe, there would be some pressure drop known as friction loss due to the internal friction of the fluid and the friction between the fluid and the wall. This friction loss directly affects the selection of the size and power of the pump and the selection of the pipe diameter. The friction factor is directly proportional to the pressure drop induced by the fluid friction.

Nusselt Number and convection heat transfer

The increase of turbulence in the fluid flow is one of the effective factors on improving heat transfer. The nature of the flow becomes more turbulent by increasing the Reynolds number. Hence, the thickness of the boundary layer decreases and the temperature gradient increases remarkably. Furthermore, the presence of graphene oxide nanoparticles with high thermal conductivity is another reason for

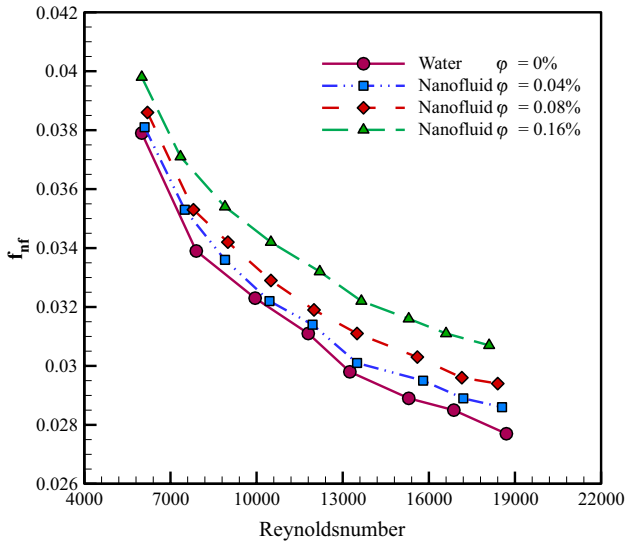

Fig. 12 Friction factor at various volume fractions vs. Reynolds number

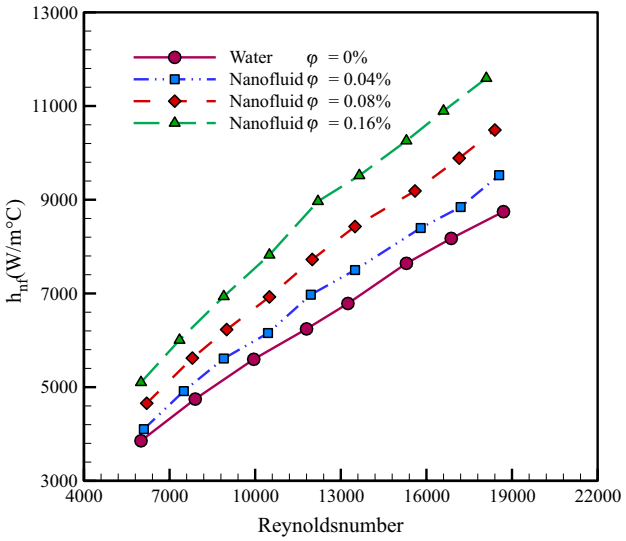

Fig. 13 Heat transfer coefficient at various Reynolds numbers

the improvement of heat transfer in the system. Figure 13 illustrates the changes in the convection heat transfer coefficient with the increase of the Reynolds number. The convection heat transfer coefficient increases at Reynolds numbers approximately equal to the increase in the volume fraction of the nanoparticles such that the heat transfer coefficient increased by 9.71, 21.2, 34.7 percent compared to that of the base fluid respectively, at volume fractions of 0.04, 0.08 and 0.16 percent in the Reynolds number of 18,700. Increasing the volume fraction of the graphene oxide nanoparticles leads to the creation of some chains in the nanofluid that improve the heat transfer. Moreover, increasing the nanoparticles in the base fluid causes an increase in the random collisions among the particles (Brownian motion) that is among the other substantial reasons for the improvement of heat transfer and increasing the Reynolds number accentuates this effect. Increasing the Reynolds number leads to a reduction in the inertial and molecular forces among the particles at higher volume fractions and improves the heat transfer.

Figure 14 shows the Nusselt number of the nanofluid turbulent flow with respect to the Reynolds number. The results show that the greatest improvement in the Nusselt number of the nanofluid flow has been achieved at a volume fraction of 0.16. These changes are directly established under the influence of the Reynolds number and the Nusselt number. The results of the Nusselt number demonstrate that even though the nanofluid has a larger thermal conductivity but the effect of the convection heat transfer is still dominant and the Nusselt number has an ascending trend. The Nusselt number increases by 10.4% at the minimum volume fraction up to 30.3% at the maximum volume fraction.

Conclusions

The importance of energy and improvement of heat transfer is among the crucial priorities in various industrial sectors. Using the Graphene oxide/ water nanofluid as an alternative fluid evaluated and the results illustrated that this nanofluid has a high potential in heat transfer at thermal systems. The results obtained from the performed experiments are as follows:

- The results of the spectrometer (FTIR) showed that a chemical bond can be formed between the Graphene

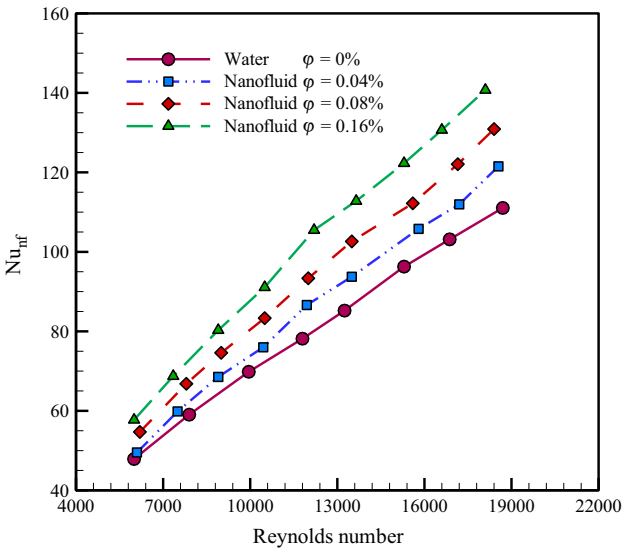

Fig. 14 Nusselt number vs. various Reynolds numbers

oxide layers and the DLS stability test confirmed the FTIR results.

- The two-step method is very appropriate for this nanofluid. The results of DLS test showed the nanoscale dimension of the particles in the base fluid.
- The rheological behavior of the nanofluid was similar to water (base fluid) and completely Newtonian under the effect of various shear rates in a range of 10–100 1/s. At the maximum volume fraction, the viscosity was increased from 0.392 mPa.s to 1.165 mPa.s at 75 ℃.
- It can be observed by investigating the hydrodynamic behavior of the internal flow that the pressure drop increases But the pressure drop is not remarkable compare to the improvement in heat transfer.
- The friction factor of the nanofluid decreases with increasing the Reynolds number and has increased by 9.64% compared to the base fluid. One of the most important parameters that affect the friction factor is the increase of the dynamic viscosity of the nanofluid.
- The heat transfer and the reduction in the temperature of the tube surface are remarkable by using the nanofluid flow. The greatest ratio of convection heat transfer has been achieved at lower Reynolds numbers. Also, the maximum increase in the Nusselt number of the flow is 30.3%. the influence of the high thermal conductivity of the Graphene oxide/ water nanofluid directly affects it.

Author contribution Ramin Ranjbarzadeh: Funding acquisition; Project administration; Writing—review & editing, Alireza Akhgar: Formal analysis; Writing—review & editing; Supervision; Methodology, Roozbeh Taherialekouhi: Conceptualization; Writing—original draft, Annunziata D'Orazio: Methodology; Writing—original draft; Validation, S. Mohammad Sajadi: Resources; Writing—original draft, Ferial Ghaemi: Writing—original draft; Validation; Conceptualization, Dumitru Baleanu: Resources; Writing—original draft; Data curation; Supervision.

References

1. Jafaryar M, Sheikholeslami M, Li Z. CuO-water nanofluid flow and heat transfer in a heat exchanger tube with twisted tape turbulator. Powder Technol. 2018;336:131–43.
2. Akyürek EF, Geliş K, Şahin B, Manay E. Experimental analysis for heat transfer of nanofluid with wire coil turbulators in a concentric tube heat exchanger. Results Phys. 2018;9:376–89.
3. Liu S, Sakr M. A comprehensive review on passive heat transfer enhancements in pipe exchangers. Renew Sustain Energy Rev. 2013;19:64–81.
4. Dogan M, İgci AA. An experimental comparison of delta winglet and novel type vortex generators for heat transfer enhancement in a rectangular channel and flow visualization with stereoscopic PIV. Int J Heat Mass Transf. 2021;164:120592.
5. Zhu C-Y, Guo Y, Yang H-Q, Ding B, Duan X-Y. Investigation of the flow and heat transfer characteristics of helium gas in printed circuit heat exchangers with asymmetrical airfoil fins. Appl Therm Eng. 2021;186:116478.
6. Mousa MH, Miljkovic N, Nawaz K. Review of heat transfer enhancement techniques for single phase flows. Renew Sustain Energy Rev. 2021;137:110566.
7. Ranjbarzadeh R, Meghdadi Isfahani AH, Hojaji M. Experimental investigation of heat transfer and friction coefficient of the water/graphene oxide nanofluid in a pipe containing twisted tape inserts under air cross-flow. Exp Heat Transf. 2018;31:373–90.
8. Mozaffari M, Karimipour A, D'Orazio A. Increase lattice Boltzmann method ability to simulate slip flow regimes with dispersed CNTs nanoadditives inside. J Therm Anal Calorim. 2019;137:229–43.
9. Khan IA. Experimental validation of enhancement in thermal conductivity of titania/water nanofluid by the addition of silver nanoparticles. Int Commun Heat Mass Transf. 2021;120:104910.
10. Choi SU, Eastman JA. Eastman, Enhancing thermal conductivity of fluids with nanoparticles, in, Argonne National Lab., IL (United States); 1995
11. Pandey RP, Shukla G, Manohar M, Shahi VK. Graphene oxide based nanohybrid proton exchange membranes for fuel cell applications: an overview. Adv Coll Interface Sci. 2017;240:15–30.
12. Dikin DA, Stankovich S, Zimney EJ, Piner RD, Dommett GH, Evmenenko G, Nguyen ST, Ruoff RS. Preparation and characterization of graphene oxide paper. Nature. 2007;448:457–60.
13. Bashirnezhad K, Ghavami M, Alrashed AA. Experimental investigations of nanofluids convective heat transfer in different flow regimes: A review. J Mol Liq. 2017;244:309–21.
14. Qi C, Luo T, Liu M, Fan F, Yan Y. Experimental study on the flow and heat transfer characteristics of nanofluids in double-tube heat exchangers based on thermal efficiency assessment. Energy Conversi Manag. 2019;197:111877.
15. Sadeghinezhad E, Mehrali M, Rosen MA, Akhiani AR, Latibari ST, Mehrali M, Metselaar HSC. Experimental investigation of the effect of graphene nanofluids on heat pipe thermal performance. Appl Therm Eng. 2016;100:775–87.
16. Ranjbarzadeh R, Karimipour A, Afrand M, Isfahani AHM, Shirneshan A. Empirical analysis of heat transfer and friction factor of water/graphene oxide nanofluid flow in turbulent regime through an isothermal pipe. Appl Therm Eng. 2017;126:538–47.
17. Prasad PD, Gupta A. Experimental investigation on enhancement of heat transfer using Al2O3/water nanofluid in a u-tube with twisted tape inserts. Int Commun Heat Mass Transf. 2016;75:154–61.
18. Yarmand H, Gharehkhani S, Shirazi SFS, Amiri A, Alehashem MS, Dahari M, Kazi S. Experimental investigation of thermophysical properties, convective heat transfer and pressure drop of functionalized graphene nanoplatelets aqueous nanofluid in a square heated pipe. Energy Convers Manage. 2016;114:38–49.
19. Devireddy S, Mekala CSR, Veeredhi VR. Improving the cooling performance of automobile radiator with ethylene glycol water based TiO2 nanofluids. Int Commun Heat Mass Transfer. 2016;78:121–6.
20. Kumar V, Tiwari AK, Ghosh SK. Characterization and performance of nanofluids in plate heat exchanger. Mater Today: Proc. 2017;4:4070–8.
21. Sarafraz M, Nikkhah V, Nakhjavani M, Arya A. Thermal performance of a heat sink microchannel working with biologically produced silver-water nanofluid: experimental assessment. Exp Thermal Fluid Sci. 2018;91:509–19.
22. Kumar NR, Bhramara P, Addis BM, Sundar LS, Singh MK, Sousa AC. Heat transfer, friction factor and effectiveness analysis of Fe3O4/water nanofluid flow in a double pipe heat exchanger with return bend. Int Commun Heat Mass Transfer. 2017;81:155–63.

23. Bergman TL, Incropera FP, DeWitt DP, Lavine AS. Fundamentals of heat and mass transfer. United States: John Wiley & Sons; 2011.
24. Pak BC, Cho YI. Hydrodynamic and heat transfer study of dispersed fluids with submicron metallic oxide particles. Exp Heat Transf Int J. 1998;11:151–70.
25. Bergman TL, Incropera FP, Lavine AS, Dewitt DP. Introduction to heat transfer. United States: John Wiley & Sons; 2011.
26. Moffat RJ. Describing the uncertainties in experimental results. Exp Thermal Fluid Sci. 1988;1:3–17.
27. Winterton RH. Where did the Dittus and Boelter equation come from? Int J Heat Mass Transf. 1998;41:809–10.
28. Aboutalebi SH, Gudarzi MM, Zheng QB, Kim JK. Spontaneous formation of liquid crystals in ultralarge graphene oxide dispersions. Adv Func Mater. 2011;21:2978–88.
29. Javidparvar AA, Naderi R, Ramezanzadeh B, Bahlakeh G. Graphene oxide as a pH-sensitive carrier for targeted delivery of eco-friendly corrosion inhibitors in chloride solution: experimental and theroretical investigations. J Ind Eng Chem. 2019;72:196–213.
30. Zhu Y, Murali S, Cai W, Li X, Suk JW, Potts JR, Ruoff RS. Graphene and graphene oxide: synthesis, properties, and applications. Adv Mater. 2010;22:3906–24.
31. El Ghandoor H, Zidan H, Khalil MM, Ismail M. Synthesis and some physical properties of magnetite (Fe3O4) nanoparticles. Int J Electrochem Sci. 2012;7:5734–45.
32. Ranjbarzadeh R, Akhgar A, Musivand S, Afrand M. Effects of graphene oxide-silicon oxide hybrid nanomaterials on rheological behavior of water at various time durations and temperatures: synthesis, preparation and stability. Powder Technol. 2018;335:375–87.
33. Ranjbarzadeh R, Isfahani AM, Afrand M, Karimipour A, Hojaji M. An experimental study on heat transfer and pressure drop of water/graphene oxide nanofluid in a copper tube under air cross-flow: applicable as a heat exchanger. Appl Therm Eng. 2017;125:69–79.
34. Newton RG Scattering theory of waves and particles. Springer Science & Business Media. 2013
35. Xuan Y, Li Q. Heat transfer enhancement of nanofluids. Int J Heat Fluid Flow. 2000;21:58–64.
36. Ahmadi MH, Mohseni-Gharyehsafa B, Ghazvini M, Goodarzi M, Jilte RD, Kumar R. Comparing various machine learning approaches in modeling the dynamic viscosity of CuO/water nanofluid. J Therm Anal Calorim. 2020;139(4):2585–99.
37. Bahiraei M, Jamshidmofid M, Goodarzi M. Efficacy of a hybrid nanofluid in a new microchannel heat sink equipped with both secondary channels and ribs. J Mol Liq. 2019;273:88–98.
38. Bahmani MH, Sheikhzadeh G, Zarringhalam M, Akbari OA, Alrashed AA, Shabani GAS, Goodarzi M. Investigation of turbulent heat transfer and nanofluid flow in a double pipe heat exchanger. Adv Powder Technol. 2018;29(2):273–82.
39. Giwa SO, Sharifpur M, Goodarzi M, Alsulami H, Meyer JP. Influence of base fluid, temperature, and concentration on the thermophysical properties of hybrid nanofluids of alumina–ferrofluid: experimental data, modeling through enhanced ANN, ANFIS, and curve fitting. J Therm Anal Calorim. 2021;143(6):4149–67.
40. Bagherzadeh SA, Jalali E, Sarafraz MM, Akbari OA, Karimipour A, Goodarzi M, Bach QV. Effects of magnetic field on micro cross jet injection of dispersed nanoparticles in a microchannel. Int J Numer Methods Heat Fluid Flow. 2019
41. Bagherzadeh SA, D'Orazio A, Karimipour A, Goodarzi M, Bach QV. A novel sensitivity analysis model of EANN for F-MWCNTs–Fe3O4/EG nanofluid thermal conductivity: outputs predicted analytically instead of numerically to more accuracy and less costs. Phys A. 2019;521:406–15.
42. Sarafraz MM, Tian Z, Tlili I, Kazi S, Goodarzi M. Thermal evaluation of a heat pipe working with n-pentane-acetone and n-pentane-methanol binary mixtures. J Therm Anal Calorim. 2020;139(4):2435–45.
43. Khosravi R, Rabiei S, Khaki M, Safaei MR, Goodarzi M. Entropy generation of graphene–platinum hybrid nanofluid flow through a wavy cylindrical microchannel solar receiver by using neural networks. J Therm Anal Calorim. 2021;1–19.
44. Abuldrazzaq T, Togun H, Alsulami H, Goodarzi M, Safaei MR. Heat transfer improvement in a double backward-facing expanding channel using different working fluids. Symmetry. 2020;12(7):1088.
45. Peng Y, Parsian A, Khodadadi H, Akbari M, Ghani K, Goodarzi M, Bach QV. Develop optimal network topology of artificial neural network (AONN) to predict the hybrid nanofluids thermal conductivity according to the empirical data of Al2O3–Cu nanoparticles dispersed in ethylene glycol. Phys A: Stat Mech Appl. 2020;549:124015.
46. Ahmadi AA, Arabbeiki M, Ali HM, Goodarzi M, Safaei MR. Configuration and optimization of a minichannel using water–alumina nanofluid by non-dominated sorting genetic algorithm and response surface method. Nanomaterials. 2020;10(5):901.
47. Dadsetani R, Sheikhzadeh GA, Safaei MR, Leon AS, Goodarzi M. Cooling enhancement and stress reduction optimization of disk-shaped electronic components using nanofluids. Symmetry. 2020;12(6):931.
48. Abdulrazzaq T, Togun H, Goodarzi M, Kazi SN, Ariffin MKA, Adam NM, Hooman K. Turbulent heat transfer and nanofluid flow in an annular cylinder with sudden reduction. J Therm Anal Calorim. 2020;141(1):373–85.
49. Akkoli KM, Banapurmath NR, Shivashimpi MM, Soudagar MEM, Badruddin IA, Alazwari MA, Yaliwal VS, Mujtaba MA, Akram N, Goodarzi M, Safaei MR. Effect of injection parameters and producer gas derived from redgram stalk on the performance and emission characteristics of a diesel engine. Alex Eng J. 2021;60(3):3133–42.
50. Safaei MR, Tlili I, Gholamalizadeh E, Abbas T, Alkanhal TA, Goodarzi M, Dahari M. Thermal analysis of a binary base fluid in pool boiling system of glycol–water alumina nano-suspension. J Therm Anal Calorim. 2021;143(3):2453–62.
51. Nguyen Q, Beni MH, Parsian A, Malekahmadi O, Karimipour A. Discrete ordinates thermal radiation with mixed convection to involve nanoparticles absorption, scattering and dispersion along radiation beams through the nanofluid. J Therm Anal Calorim. 2021;143(3):2801–24.
52. Zheng Y, Zhang X, Nouri M, Amini A, Karimipour A, Hekmatifar M, Sabetvand R, Ngooyen Q, Karimipour A. Atomic rheology analysis of the external magnetic field effects on nanofluid in non-ideal microchannel via molecular dynamic method. J Therm Anal Calorim. 2021;143(2):1655–63.
53. Yan SR, Kalbasi R, Parvin A, Tian XX, Karimipour A. Comparison of Nusselt number and stream function in tall and narrow enclosures in the mixed convection of hybrid nanofluid. J Therm Anal Calorim. 2021;143:1599–609.
54. Niknejadi M, Afrand M, Karimipour A, Shahsavar A, Isfahani AHM. Experimental investigation of the hydrothermal aspects of water–Fe 3 O 4 nanofluid inside a twisted tube. J Therm Anal Calorim. 2020;143(1):801–10.
55. Liu X, Toghraie D, Hekmatifar M, Akbari OA, Karimipour A, Afrand M. Numerical investigation of nanofluid laminar forced convection heat transfer between two horizontal concentric cylinders in the presence of porous medium. J Therm Anal Calorim. 2020;141(5):2095–108.
56. Zheng Y, Yaghoubi S, Dezfulizadeh A, Aghakhani S, Karimipour A, Tlili I. Free convection/radiation and entropy generation

analyses for nanofluid of inclined square enclosure with uniform magnetic field. J Therm Anal Calorim. 2020;141(1):635–48.
57. Yan SR, Kalbasi R, Nguyen Q, Karimipour A. Rheological behavior of hybrid MWCNTs-TiO2/EG nanofluid: a comprehensive modeling and experimental study. J Mol Liq. 2020;308:113058.
58. Tian XX, Kalbasi R, Qi C, Karimipour A, Huang HL. Efficacy of hybrid nano-powder presence on the thermal conductivity of the engine oil: an experimental study. Powder Technol. 2020;369:261–9.
59. Salimpour MR, Darvanjooghi MHK, Abdollahi A, Karimipour A, Goodarzi M. Providing a model for Csf according to pool boiling convection heat transfer of water/ferrous oxide nanofluid using sensitivity analysis. Int J Numer Method Heat Fluid Flow. 2019;30(6):2867–81.
60. Tian Z, Bagherzadeh SA, Ghani K, Karimipour A, Abdollahi A, Bahrami M, Safaei MR. Nonlinear function estimation fuzzy system (NFEFS) as a novel statistical approach to estimate nanofluids' thermal conductivity according to empirical data. Int J Numer Method Heat Fluid Flow. 2019;30(6):3267–81.
61. Yan SR, Shirani N, Zarringhalam M, Toghraie D, Nguyen Q, Karimipour A. Prediction of boiling flow characteristics in rough and smooth microchannels using molecular dynamics simulation: Investigation the effects of boundary wall temperatures. J Mol Liq. 2020;306:112937.
62. Ma J, Shahsavar A, Al-Rashed AA, Karimipour A, Yarmand H, Rostami S. Viscosity, cloud point, freezing point and flash point of zinc oxide/SAE50 nanolubricant. J Mol Liq. 2020;298:112045.
63. Abu-Hamdeh NH, Alsulami RA, Alimoradi A, Karimipour A. Fluid flow and heat transfer of the two-phase solid/liquid mixture at the equilibration phase structure via MD method: Atomic value effects in a case study of energy consumption and absorbed energy. J Mol Liq. 2021;337:116384.
64. Alazwari MA, Abu-Hamdeh NH, Nusier OK, Karimipour A. Vacancy defect influence on nanofluid flow and absorbed thermal energy in a nanochannel affected by universal force field via composed approach of embedded atom model/molecular dynamics method. J Mol Liq. 2021;333:115927.
65. Bantan RA, Abu-Hamdeh NH, Nusier OK, Karimipour A. The molecular dynamics study of aluminum nanoparticles effect on the atomic behavior of argon atoms inside zigzag nanochannel. J Mol Liq. 2021;331:115714.

Publisher's Note Springer Nature remains neutral with regard to jurisdictional claims in published maps and institutional affiliations.